Laser and Particle Beams (2007), *25*, 127–141. Printed in the USA.

DOI: 10.1017/S0263034607070164

Recent experiments on the hydrodynamics of laser-produced plasmas conducted at the PALS laboratory

D. BATANI,[1] R. DEZULIAN,[1] R. REDAELLI,[1] R. BENOCCI,[1] H. STABILE,[1] F. CANOVA,[1] T. DESAI,[1] G. LUCCHINI,[1] E. KROUSKY,[2] K. MASEK,[2] M. PFEIFER,[2] J. SKALA,[2] R. DUDZAK,[2] B. RUS,[2] J. ULLSCHMIED,[2] V. MALKA,[3] J. FAURE,[3] M. KOENIG,[4] J. LIMPOUCH,[5] W. NAZAROV,[6] D. PEPLER,[7] K. NAGAI,[8] T. NORIMATSU,[8] AND H. NISHIMURA[8]

[1]Dipartimento di Fisica "G. Occhialini," University of Milano Bicocca, Milan, Italy
[2]PALS Centre, Academy of Sciences, Prague, Czech Republic
[3]LOA, Ecole Politechnique, CNRS, Palaiseau, France
[4]LULI, Ecole Politechnique, CNRS, Palaiseau, France
[5]Czech Technical University, Praha, Czech Republic
[6]University of St. Andrews, Scotland, UK
[7]Central Laser Facility, CCLRC Rutherford Appleton Laboratory, UK
[8]ILE, Osaka University, 2-6 Yamadaoka, Suita City, Osaka 565-0871, Japan

(RECEIVED 1 October 2006; ACCEPTED 29 October 2006)

Abstract

We present a series of experimental results, and their interpretation, connected to various aspects of the hydrodynamics of laser produced plasmas. Experiments were performed using the Prague PALS iodine laser working at 0.44 μm wavelength and irradiances up to a few 10^{14} W/cm^2. By adopting large focal spots and smoothed laser beams, the lateral energy transport and lateral expansion have been avoided. Therefore we could reach a quasi one-dimensional regime for which experimental results can be more easily and properly compared to available analytical models.

Keywords: Equation of State; Laboratory Astrophysics; Plasma Hydrodynamics; Shock Acceleration; Shock Pressure; Smoothing

INTRODUCTION

The hydrodynamics of laser produced plasmas is a field which is of interest both in itself (for the study of fluid dynamics of plasmas) and for its various applications, starting with inertial confinement fusion (ICF) of thermonuclear targets (Chizkhov *et al*., 2005; Gus'Kov, 2005; Kilkenny *et al*., 2005; Koresheva *et al*., 2005) continuing with the physics of shock waves (Pant *et al*., 2006), the realization of huge pressures and of extreme states of matter (Hoffmann *et al*., 2005), the study of hydrodynamics instabilities (Rayleigh–Taylor to start with) (Piriz *et al*., 2006; Fincke *et al*., 2005), and the study of laser-matter interaction including the problems of energy transport and smoothing of energy deposition (Hora, 2006).

All of these topics have been the subject of intense research starting from the 1970s in the context of laser-matter interaction. Despite this, there are still some very good and important reasons to continue and update such research. Indeed, progress in laser technology have allowed new regimes to be obtained (especially the fact that much higher laser intensities are available today) and also to realize *cleaner* experiments, which allows for conditions closer to those for which theoretical models have been derived. In particular, laser-smoothing techniques have been introduced in the 1980s, and in the 1990s allow the realization of improved irradiation conditions. Indeed it turns out that most past studies were done by focusing the laser energy to small focal spots in order to achieve intensities of 10^{13}–10^{15} W/cm^2. Thereby, experimental results were affected by strong two-dimensional (2D) effects (lateral transport of thermal energy, lateral flow of mass).

Even when large spots were used, these were not optically smoothed (the first smoothing technique, random phase plates (RPP), was introduced in 1980 (Kato *et al*., 1984)), and were then characterized by the presence of "hot spots" in the intensity profile. The effects of short-scale inhomogeneities therefore often dominated the measured parameters.

Address correspondence and reprint requests to: Dimitri Batani, Dipartimento di Fisica "G. Occhialini," University of Milano Bicocca, Milan, Italy. E-mail: batani@mib.infn.it

Among optical smoothing techniques, the use of phase zone plate (PZP) optical smoothing (Stevenson *et al*., 1994; Batani *et al*., 2002*a*; see next section) has allowed a flat-top intensity distribution to be produced. This is important since the parameters in the central flat region of the focal spot can be directly compared to analytical results obtained from one-dimensional (1D) models, which very often by definition assume a spatially uniform intensity.

In this paper, we will present a series of experiments respectively dedicated to the study of shock (ablation) pressures vs. laser intensity; the generation of extreme states of matter by laser compression, and the application to the study of equation of state (EOS) of material in the Mbar pressure range (here we used carbon); the study of shock acceleration in foams (a problem which is important also in connection to astrophysical situations); and finally the study of smoothing of laser energy deposition by foams and gas jets.

All experiments were performed using the Prague PALS iodine laser working at 0.44 μm wavelength and irradiances up to a few 10^{14} W/cm^2, and by applying optical smoothing techniques.

EXPERIMENTAL SET-UP

The iodine laser of PALS (Jungwirth *et al*., 2001, Jungwirth, 2005; Batani *et al*., 2004*a*; Koenig *et al*., 1994) delivers a single beam, 29 cm in diameter, with energies up to 250 J per pulse at 0.44 μm. The laser pulse is Gaussian in time with a full width at half maximum (FWHM) of 350 ps. The schematic experimental set-up is shown in Figure 1. The focusing lens had a focal length $f = 600$ mm ($f/2$ aperture). A blue filter before the entrance window did cut ω and 2ω light.

In all experiment, we used a time-resolved *self-emission* diagnostics. Such a diagnostics was used to detect the shock breakout from the target rear face and consisted in a pair of lenses imaging the rear face onto the slit of a streak camera (Hamamatsu C7700 with S-1 photocathode). The first one was a complex $f/2$ objective, with $f = 100$ mm, producing a parallel beam between the two lenses. A red filter RG60 before the streak camera cut out any 3ω light. The second lens had $f = 98$ cm, giving a total optical magnification $M = 9.8$. The CCD had 512×512 pixel and 16 bits dynamic range. The spatial resolution was measured to be 2.6 μm/pixel, and the temporal resolution 3.12 ps/pixel (choosing a 1600 ps time window). Also in all experiments (except those on smoothing presented in Section 5 of this paper), we used PZP (Stevenson *et al*., 1994; Batani *et al*., 2002*a*) with the goal of producing uniform irradiation conditions. In this case, the intensity distribution is characterized by a central flat-top region with Gaussian wings.

In our experiment, the PZP, half of the laser beam size, was placed at $f/2$ from target. The characteristics of our optical system (PZP + focusing lens) implied a focal spot of 560 μm FWHM, with a 400 μm flat central region, corresponding to peak intensities up to 2.4×10^{14} W/cm^2.

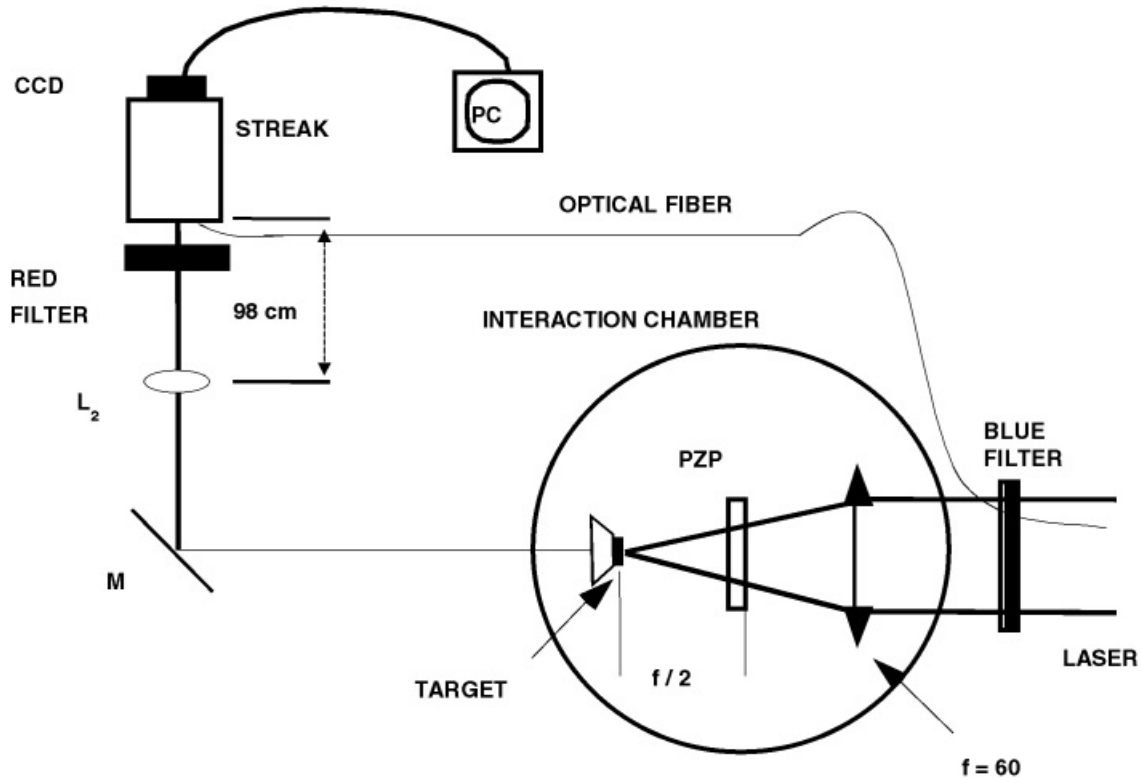

Fig. 1. Experimental set-up at PALS.

https://doi.org/10.1017/S0263034607070164 Published online by Cambridge University Press

In reality, the intensity profile produced by PZPs is not really flat but characterized by small scale length speckles (of typical dimension less than 10 μm). However, small speckles are rapidly washed away by thermal smoothing (Batani *et al*., 2000*a*), so they are not expected to influence our measurements. In any case, the spatial and temporal resolution of our diagnostics is not sufficient to see such effects. The effects of speckles on shock breakout were observed by Benuzzi-Mounaix *et al*. (1999) by using a diagnostics with higher space and time resolution. However, it was not large, inducing local differences in shock breakout time in the order of 10 ps, which does not appreciably influence our measurement of shock velocity (which is determined by a shock transit time in the step of the order of 1 ns).

SCALING OF SHOCK PRESSURE WITH LASER INTENSITY

The process of laser ablation of low- and medium-Z targets is fundamental for laser-driven IFC since it is the source of the driving pressure in ablative compression of fusion targets. In particular, studies have focused on establishing the scaling laws vs. laser intensity and laser wavelength, to be used as a guide in the selection of laser parameters, in order to obtain the highest hydrodynamic efficiency in laser-driven implosions.

As recalled before, the progress in laser technology, and in particular the introduction of smoothing techniques, allows cleaner experiments to be performed and justifies the interest in the field. However there are also other more specific reasons:

(1) At the shortest laser wavelengths, there is still some incertitude concerning the scaling vs. laser intensity. For instance, measurements at 0.351 μm by Key *et al*. (1980, 1983) showed a scaling $\approx I^{0.3}$, very different from what was predicted by various theoretical models (usually $\approx I^{0.7}$). 2D and drilling effects dominated indeed such experimental results. Also, to our knowledge, data for 0.351 μm laser ablation of Al targets in the range 10^{13} to 10^{14} W/cm^2 have not been reported. This is important because shorter laser wavelengths (third and fourth harmonics of Nd, as well as other wavelengths from gas lasers) have the advantage of giving higher ablation rate and pressure, and are thereby envisaged as future drivers for ICF direct drive experiments (Koenig *et al*., 1992).

(2) Still some details are not clear in the literature concerning the very mechanism of laser ablation. For instance, even recent important reviews (Lindl, 1995) report the scaling law:

$$P\,(\mathrm{Mbar}) = 8.6\,(I/10^{14})^{2/3}\lambda^{-2/3}(A/2Z)^{1/3,} \qquad (1)$$

where I is the laser intensity on target in W/cm^2, λ is the laser wavelength in μm, and A and Z are the mass number and the atomic number of the target. This is obtained by considering that laser light is absorbed at the plasma critical layer.

In reality, the mass ablation rate scaling should also include a time dependence. Indeed the plasma corona size becomes larger during the interaction, and the distance between the absorption region and the ablation surface ($n_e \approx$ solid material) increases with time. This brings to a decoupling of the laser beam from the target and, as a result, the mass ablation rate decreases with time. In particular, it is found that the shock pressure is related to laser and target parameters by (Mora, 1982):

$$P\,(\mathrm{Mbar}) = 11.6(I/10^{14})^{3/4}\lambda^{-1/4}(A/2Z)^{7/16}(Z^*t/3.5)^{-1/8}, \qquad (2)$$

where the time t is in ns and Z^* is the average ionization degree in the plasma corona. As with the previous scaling law (Eq. (1)), pressure strongly depends on laser parameters and only weakly on the material. The decrease in time of ablation pressure, even for constant laser irradiation, has been first described by Caruso and Gratton (1968) and later by Mora (1982). The difference between de-localized absorption and localized (at critical density) models is discussed in detail by Meyer and Thiell (1984).

In order to address such questions, we performed an experiment at the PALS laboratory, using beam-smoothing in order to avoid the "drilling effect" from hot spots (Lebo *et al*., 1999). In the past, several experimental techniques have been used in order to measure the mass ablation rate and pressure (see Batani *et al*. (2003*a*) for a brief introduction). Here we obtained the shock (ablation) pressure from the experimental measurement of shock velocity, taking advantage of the recent advancement in the generation of high quality shocks, and in the measurements of shock velocities with stepped targets (Koenig *et al*., 1995; Batani *et al*., 2000*b*, 2003*b*). As compared to other methods, this is a quite direct measurement of ablation pressure, and less prone to 2D effects (since we measure shock velocity in the central region of the focal spot where shock dynamics is practically 1D thanks to the use of PZPs, and since the measurement takes place at very early times).

Figure 2 shows a streak image of shock breakout from an Al flat target and from an Al stepped target. The first image shows that indeed by using PZPs it is possible to get quite uniform shocks. The second image allows calculating the shock velocity in the material (Al): the time delay between the breakout at the base and at the step gives the average shock velocity in the step. From the shock velocity we determine the shock pressure using the Huguenot data for Al from the Sesame tables (SESAME, 1983). Such shock pressure is the pressure produced by the laser beam on the irradiation side, i.e., the ablation pressure. The method works if the shock is stationary, and we designed the targets to get a stationary shock in the step. This can be addressed by using hydrodynamics simulations or analytical models (Batani *et al*., 2001, 2003*b*), which approximate the Gaussian with a trapezoidal time shape.

https://doi.org/10.1017/S0263034607070164 Published online by Cambridge University Press

Fig. 2. Left: shock breakout from a flat aluminum target. Image 1.69 ns × 1300 μm; **Right**: Shock breakout image from an Al target for laser energy $E_L = 108$ J. The dimensions of the images are 1.69 ns × 1300 μm. Times flows up to down. The time delay between base and step is $\Delta t = 267$ ps giving a shock velocity $D = 31.84$ μm/ns.

Typical errors were calculated by considering the error on target thickness (including surface roughness), the streak camera resolution, as determined by the time window (1.69 ns), and the slit size (115 μm), and the error in data reading. The error on shock velocity D was then propagated, giving a ±20% error bar on the pressure.

The laser intensity on target is obtained by measuring the laser energy shot by shot (through a calibrated reflection from the entrance window of the chamber) and includes the losses (about 20%) due to the use of PZPs. Also it is calculated taking into account the flat-top intensity profile, i.e., it corresponds to the effective intensity in the central region of the focal spot. As for the time dependence, the x-axis in Figure 3 reports the time-averaged intensity over the laser pulse duration.

Figure 3 summarizes our experimental results for ablation pressure vs. laser intensity on target. It also shows two theoretical curves corresponding to the law given by Mora (1982):

$$P\,(\text{Mbar}) = 12\,(I/10^{14})^{2/3}\lambda^{-2/3}(A/2Z)^{1/2}. \tag{3}$$

This corresponds to Eq. (1) except for the factor 12, which was originally derived theoretically (Fabbro *et al.*, 1982, 1985; Garban-Labaune *et al.*, 1985). The interpolation of experimental data with Mora's law requires some care. Indeed in the case of delocalized absorption, the shock pressure (and shock velocity) decrease with time. Hence weaker shocks, produced at lower intensities, travel more slowly in the target and breakout later; thereby they have more time to slow down. Shock velocity is measured at shock breakout, but the shock breakout time (the time t to be inserted in Eq. (2)) is different for low and high laser intensity.

In order to take this effect into account, we write that

$$d = \int D(t)\,dt, \tag{4}$$

where d is the target thickness, and the time integral goes from 0 to the breakout time.

$$D = \left(\frac{(\gamma+1)}{2}\,\frac{P}{\rho_0}\right)^{1/2} \tag{5}$$

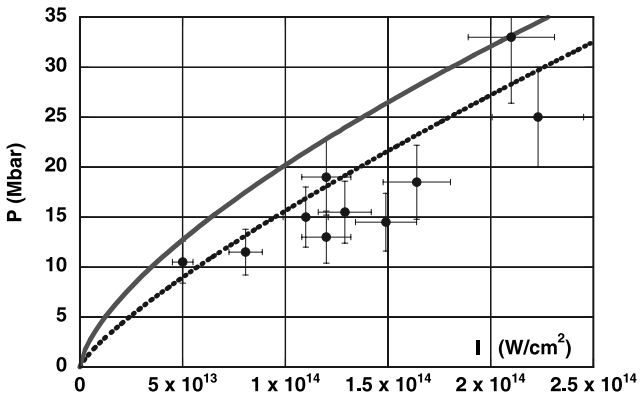

Fig. 3. Our experimental results (dots) with scaling laws for absorption at the critical density (Lindl, 1995; continuous line, Eq. (3)), and delocalized absorption (Mora, 1982; dotted line, Eq. (6)).

https://doi.org/10.1017/S0263034607070164 Published online by Cambridge University Press

The relation between the shock velocity D and the shock pressure P is (Zeldovich & Raizer, 1967) where γ is the adiabatic constant of the material and ρ_o is the unperturbed target density ($\rho_o = 2.7$ g/cm^3 for Al). Eqs. (4) and (5) allow the shock breakout time to be determined, and by inserting it into Eq. (2) we finally get an equation, which is formally independent of time, but dependent on target thickness, i.e.:

$$P\,(\text{Mbar}) = 15.63(I/10^{14})^{0.8}\lambda^{-4/15}\rho_o^{-1/15}d^{-2/15}, \qquad (6)$$

where d is in μm and where the coefficient was calculated for $A = 27$ and $Z = Z^* = 13$ (however, the dependence on the ionization degree Z^* is practically negligible). Here we simplified the calculation by assuming an "average" thickness $d = (d_{\text{base}} + d_{\text{step}}/2)$. This may be done because the time exponent in Mora's law (0.125) is very small, i.e., the shock decreases quite slowly with time. As can be seen, our experimental data are close to Mora's law, as compared with Eq. (3). This concerns not only the values of pressures but also the scaling vs. laser intensity. From this point of view, substituting the factor 12.3 with the factor 8.6, i.e., using Eq. (1) instead of Eq. (3) may be a tentative of fitting the theoretical scaling obtained for localized absorption with experimental data.

In summary, the laser ablation pressure at 0.44 μm has been measured in planar Al targets at irradiance up to 2×10^{14} W/cm^2. By adopting relatively large focal spots and a smoothed laser beam, the later energy transport and the "drilling effect" were avoided. Our results show a scaling vs. laser intensity, which is quite close to the theoretical prediction and gives some evidence for the mechanism of delocalized absorption.

EQUATION OF STATE OF CARBON

In the Megabar pressure range, extreme states of matter are reached and many materials undergo interesting phase transitions. For instance, materials like hydrogen and carbon are expected to become metals. The knowledge of such states of matter, and in particular, of the equation of states of materials, are of extreme importance in astrophysics and planetology since pressures of several Megabars or tens of Megabars are indeed reached in the interior of planets, giant planets, and brown dwarfs.

High-energy lasers are nowadays the only laboratory tool, which can achieve pressures of a few tens of Mbars (Lindl, 1995; Mora, 1982). In recent years, it has been well established that laser-shocks are a useful tool for high-pressure physics, to compress materials at Megabar pressures and measure their EOS (Koenig *et al*., 1995; Batani *et al*., 2000*b*, 2002*b*; Gupta & Sharma, 1997).

One particularly interesting material is carbon. Its EOS at high pressures (Megabar or Multi-Megabar regime) is of interest for several branches of physics, namely:

(1) Material science: carbon is a unique element due to its polymorphism and the complexity and variety of its state phases. The EOS of carbon has been the subject of several recent important experimental and theoretical scientific works (Fahy & Louie, 1987; Ruoff & Luo, 1991; Mao & Bell, 1978, 1979; Mao & Hemley, 1991; Bundy, 1963; 1989, Bundy *et al*., 1973; Grumbach & Martin, 1996; Sekine, 1999; Benedetti *et al*., 1999; Scandolo *et al*., 1996; Cavalleri *et al*., 2002). The important phenomenon of carbon metallization at high pressure has long been predicted theoretically but until now never experimentally proved. At very high pressures the regime of non-ideal strongly-correlated and partially-degenerate plasmas is approached, which is characterized by an almost complete absence of experimental data; in this regime, the most complete EOS are the SESAME tables developed at the Los Alamos Laboratory (SESAME, 1983; Ross, 1985; Eliezer *et al*., 1986).

(2) Astrophysics: description of high pressures phases is essential for developing realistic models of planets and stars (Saumon *et al*., 1995; Guillot, 1999). Carbon is a major constituent (through methane and carbon dioxide) of giant planets like Uranus and Neptune. High pressures are thought to produce methane pyrolisys with a separation of the carbon phase and possible formation of a diamond or metallic layer (Ross, 1981; Ancilotto *et al*., 1997; Nellis *et al*., 2001*a*). Metallization of the carbon layer in the mantle of these planets (the "ice" layers) could give high electrical conductivity and, by dynamo effect, is the source of the observed large magnetic fields (Ness *et al*., 1986; Connerney *et al*., 1987).

In Figure 4, we have reported a simplified version of Grumbach and Martin's (1996) phase diagram to which we added the Huguenot curves corresponding to the initial densities $\rho_o = 1.6$ g/cm^3 and $\rho_o = 1.45$ g/cm^3 (the two values used in our experiment), calculated following the Sesame tables. Again, the liquid metallic phases can be easily reached with laser shocks.

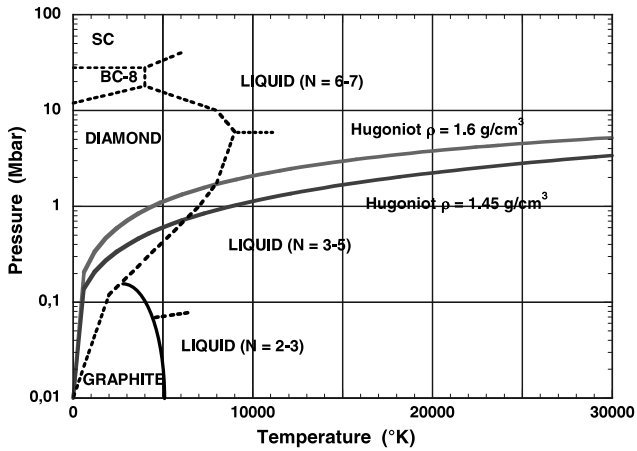

Fig. 4. Grumbach and Martin's (1996) phase diagram and the two Huguenot curves corresponding to the initial densities $\rho_o = 1.6$ g/cm^3 and $\rho_o = 1.45$ g/cm^3.

https://doi.org/10.1017/S0263034607070164 Published online by Cambridge University Press

Our group has been the first one to obtain Huguenot data for carbon with laser-driven shocks. We began the exploration of carbon EOS in the pressure range 1–15 Mbar and obtained the first experimental points at pressures higher than 8 Mbar (Batani *et al*., 2004*b*). Moreover, we substantially increased the number of EOS data for carbon at pressures $>$ 1 Mbar (Batani *et al*., 2004*b*); we presented nine new EOS points against a total of about 20 points which, to our knowledge, were available in literature (Drakin & Pavlovskii, 1966; Nellis *et al*., 2001*b*; Pavlovskii, 1971; Gust, 1980; Marsh, 1980).

One general limitation of shock-wave EOS experiments is that only data on the Huguenot curve of the material are obtained. This is due to the fact that shocks compress and heat the material at the same time, so pressure and temperature are no longer two independent variables. One way to overcome such limitation is to use a sample with reduced density ρ_o (porous or foam target). This changes the initial conditions in the material so that data along *different* Huguenot curves are obtained. Hence by changing ρ_o the whole EOS plane can be explored. In particular, by reducing the initial density ρ_o of the sample, the same shock pressure P will correspond to a higher temperature T (internal energy E) and a reduced final density ρ.

The experiment is based on generating high quality shocks and using "two steps–two materials" targets (Fig. 2). Relative EOS data of "unknown" materials (here C) are obtained by using a "well-known" reference (here Al). Al behavior at high pressure is well known, making it a typical reference material for shock experiments. The method is described in detail in by Batani *et al*. (2000*b*).

Figure 5 shows a SEM photo of the carbon steps deposited on a CH/Al substrate at the University of Milan (Barborini *et al*., 1999, 2000; Piseri *et al*., 2001). The deposition technique allowed the realization of targets with an acceptable surface roughness (less than 0.5 μm, i.e., $\approx$ 3% of step thickness which was on the order of 15 μm). These give an error comparable to the typical $\leq$ 5% due to streak camera resolution. The Al step thickness was 5 μm. Other carbon targets were fabricated at General Atomics using a completely different technique based on the use of colloidal carbon. In this case, carbon with initial density $\rho_o = 1.6 \pm 0.10$ g/cm^3 was produced. Stepped targets were made of lathe machining of bulk aluminum. The Al base was $\approx$ 8 μm, and the step thickness was $\approx$ 8,5 μm. The carbon layer was then produced and the target was machined again to produce the C step (with thickness $\approx$ 10 μm). The use of two different type of targets allow a comparison of measurements and a better confidence in our results

Figure 6 shows a typical result obtained from the emissive diagnostics. In total, we obtained two good experimental points for $\rho_o = 1.45$ g/cm^3 and seven good points for $\rho_o = 1.6$ g/cm^3. These are shown in Figure 7 with all of the other experimental results already available in the literature in the pressure range $P \geq 1.5$ Mbar. Data grouped according to their initial density ρ_o, are compared to the shock polar curve derived from the SESAME tables (the model QEOS) (More *et al*., 1988) yields practically identical results for carbon, even if usually it does not describe the Huguenot with the same accuracy like the SESAME EOS does. The errors on pressure and fluid velocity are $\approx$ 15% and $\approx$ 20%, respectively; these error bars have been estimated by calculating the propagation of experimental errors on shock velocity (5%) on the quantities determined by the mismatch

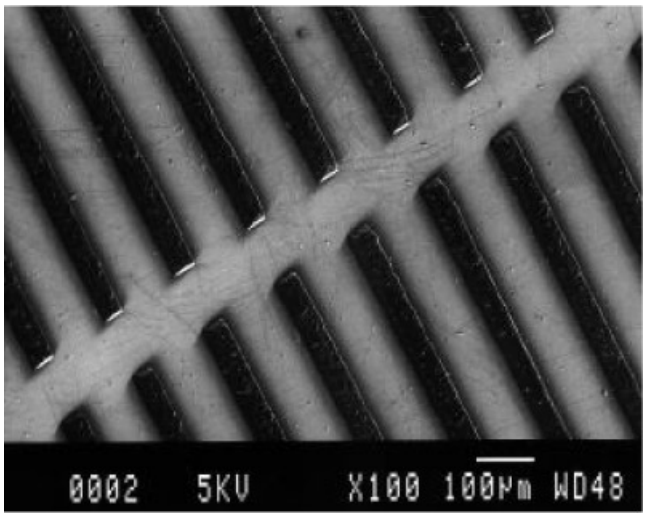

Fig. 5. SEM image of carbon steps with $\rho_o = 1.45$ g/cm^3 deposited on a CH/Al substrate. Al steps are not present since they were deposited later.

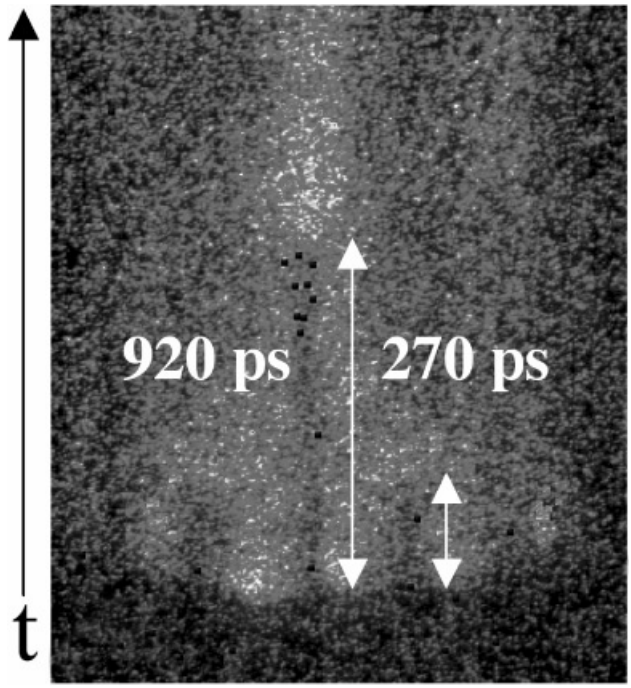

Fig. 6. Shock breakout streak image of the target rear side in emission. Shot energy was 25.3 J. Arrows indicate the shock breakout from the Al step (**right**) and from the C step (**left**). The size of the image is 600 μm $\times$ 1.7 ns.

https://doi.org/10.1017/S0263034607070164 Published online by Cambridge University Press

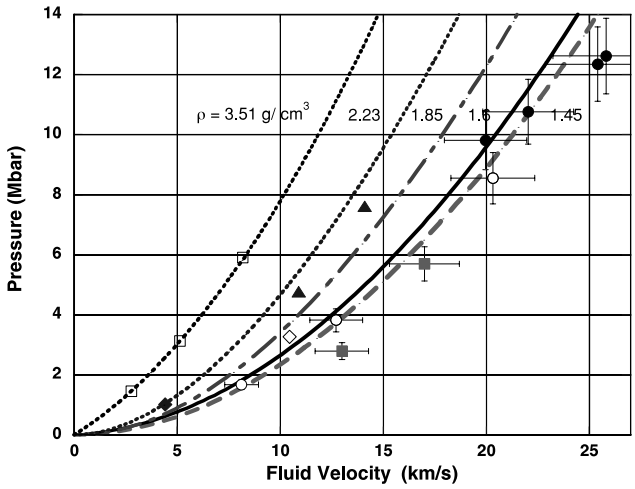

Fig. 7. Experimental EOS results from shock experiments. Only data with P ≥ 1.5 Mbar and corresponding Huguenot are shown. Our points: full squares, 1.45 g/cm^3 LULI; empty circles, 1.6 g/cm^3 LULI; full circles, 1.6 g/cm^3 PALS. Previous points: empty diamond, 1.85 g/cm^3 by Drakin and Pavlovskii (1966); triangles, 2.2 g/cm^3 by Nellis *et al.* (2001*b*); full diamond, 2.23 g/cm^3 by Drakin and Pavlovskii (1966); empty squares, 3.51 g/cm^3 (diamond) by Pavlovskii (1971).

method. The error on shock velocity is instead determined from the experimentally measured uncertainties on step thickness and by streak-camera temporal resolution.

All of our data, for both initial densities are below the shock polar curve derived from the SESAME tables. Despite our quite large error bars (which make most points compatible with the theoretical curve), such results show a systematic deviation, and indicate a compressibility of carbon, at these pressures, much higher than what predicted by most models (the density ρ of the compressed sample is obtained from the Huguenot–Rankine relations for shocks, namely from $\rho\,(D-U) = \rho_o D$). However such behavior could also be due to the presence of systematic errors in our experiment. One possible cause often cited for explaining errors in laser-shock EOS experiments is preheating induced by X-rays (Desai *et al.*, 2007). In our case, preheating was probably small due to the presence of a CH layer on laser-irradiated side, which reduces X-ray generation (as shown experimentally by Benuzzi *et al.* (1998)). Moreover, if preheating was the source of deviation, it should affect more data at higher laser intensity (higher pressure), which is not really the case. Therefore preheating is probably not the cause of deviation from theoretical curves (or at least not for the whole deviation). Another possible systematic effect could be due to the high porosity of the targets, even if porous and foam targets are routinely used in EOS experiments. Hence, even if this point requires further future work and analysis, for the moment, we can conclude that at very high pressures carbon is likely to be more compressible than predicted by SESAME or QEOS. Let's notice that a deviation from SESAME is also observed for other points obtained at high shock pressure (for instance, the point at ≈ 3 Mbar for carbon with $\rho_o =$ 1.85 g/cm^3 reported by Drakin and Pavlovskii (1966)). Even more interestingly, the same behavior was observed by Nellis *et al.* (2001*b*) who, using underground nuclear explosions as a compression tool, report two EOS points for graphite ($\rho_o = 2.2$ g/cm^3) at 4.76 and 7.61 Mbar.

The relation between shock velocity D and fluid velocity U for carbon in the Megabar range is linear ($D = C + SU$, where C is the sound velocity in the material in that pressure range). For carbon with $\rho_o = 1.6$ g/cm^3, from SESAME (or QEOS), we get $C \approx 5$ km/s and $S \approx 1.27$ (this is true for QEOS and the SESAME table 7830; other carbon tables give different, but close values). A linear interpolation of our points instead yields $S \approx 1.08$–1.14. From this we get an "experimental" shock polar $P = \rho_o DU = \rho_o U(C + SU)$ which of course nicely interpolates our results in the (P, U) plane. Such curve is above the thermodynamic limit $P = \rho_o U^2$ corresponding to infinite compressibility (all of our experimental points are above such limit). However, it seems too close to the shock polar for a perfect gas, which again could indicate an influence from systematic effects. For the case $\rho_o = 1.45$ g/cm^3 we did not make any attempt to determine S since we had two points only.

The observed increased compressibility of carbon, suggests that at a given pressure along the Huguenot, the density in the final liquid state (see Fig. 4) is smaller than that for solid. Transitions to less dense phases also enhance thermal contributions, explaining the observed pressure discrepancy. This agrees with the conclusions by Nellis *et al.* (2001*b*) and reinforces their observations.

SHOCK ACCELERATION IN FOAMS

In recent years, laser-plasmas have also been used as a tool to simulate astrophysical events in the laboratory. This has opened the new research field of "*Laboratory astrophysics*." In particular, up to now, experiments have addressed problems related to the development of hydrodynamical instabilities (Drake, 2005) (Rayleigh–Taylor instability in particular), the physics of shock waves (in particular of radiative shocks (Koenig *et al.*, 2005*a*, 2006; Vinci *et al.*, 2005; Fleury *et al.*, 2002)), the formation of astrophysical jets (Ciardi *et al.*, 2002), the EOS and opacities of materials (Eidmann *et al.*, 1998; Winhart *et al.*, 1996), etc.

In this context, we have addressed one particular problem, i.e., the acceleration of shocks as they travel in a decreasing density profile. This situation is met in the explosion of supernovae where the shock accelerates as it propagates through the less and less dense atmosphere of the supernova. As the shock accelerates, the matter behind the shock front becomes hotter and hotter and finally is so hot to give rise to a large emission of X-rays (XUV burst).

In our case, we measured the shock acceleration at the interface between two materials, with a decreasing density jump. The case of a discontinuous density jump, may somewhat be considered as the limiting case of a continuous decreasing profile, therefore it is important to validate the

https://doi.org/10.1017/S0263034607070164 Published online by Cambridge University Press

physical laws for shock propagation in such simple limiting case (Teyssier *et al*., 2000).

In our experiment, the shock accelerated when it crossed the interface between an Al layer and a very-low density material (foam). Our plastic foams were produced at the Target Material Laboratory of ILE, Osaka University, by the aerogel method, which allows the production of films with area of mm^2 order and density in the range of 50 to150 mg/cm^3 with chemical composition CH_2 (poly(4-methyl-1-pentene)). Several-ten-nanometer sized crystals are aggregated, and macroscopic-pore void size was ≤ 2 μm over an area < 1 mm^2 and for density > 50 mg/cm^3 (Nagai *et al*., 2002*a*, 2002*b*, 2004; Okihara *et al*., 2004; see Fig. 8). The foam film was put in contact with the Al foil using the single molecule glue method (Nagai *et al*., 2002*a*, 2002*b*, 2004; Okihara *et al*., 2004).

In the experiment, we used three-layer-targets. The first layer was a 4 μm plastic (CH) ablator, which was present to reduce preheating (Benuzzi *et al*., 1998). The second was a 10 μm Al foil followed by a foam layer of typical thickness 100–190 μm (the foam thickness was measured on each single sample). Such a foam layer was finally covered on half size by a thin (500 Å) Al deposition.

Our foams are transparent to visible light, and here we used their transparency to detect a shock breakout from the Al base through the foam (as previously done by Koenig *et al*. (1999*a*, 2000, 2005*b*)). However, unlike in that experiment, we did use quite thick foam layers (typically $\approx$ 100–190 μm against ≈ 20 μm). Indeed, provided the shock velocity is constant in the foam (i.e., the shock is stationary), the precision in the measurement of the shock velocity in the foam is inversely proportional to the foam thickness. However, in this case, it became impossible to use an Al stepped target as reference (as done by Koenig *et al*. (1999*a*, 2005*b*)). In fact, with thin steps (5–10 μm as in Koenig *et al*. (1999*a*, 2005*b*)) the time difference between breakout at base and step is not easily detectable on the same streak image of the foam shock breakout. On the other hand, using thick steps would imply a nonstationary shock in Al. Therefore, in our case, shock velocity was determined by measuring the time difference between shock breakout on the rear side of the Al flat layer (base), and the arrival of the laser pulse on the target front side (as determined with a time fiducial implemented through an optical fiber carrying a small part of the laser signal onto the streak camera slit, see Fig. 9).

Figure 9 shows instead a streak image from an Al/foam target (in this case only, the target front was not covered by the CH layer). All other shots were realized with a 4.9 ns window (instead of 10 ns) in order to increase the accuracy of the measurement. The left side of the target rear is covered with a very thin Al layer. When the shock reaches the Al rear side, its breakout produces a strong luminosity, which is detected through the transparent foam (but it is partially masked on the left by the thin Al layer). On the contrary, the luminosity due to the shock breakout on the foam rear side is strongly enhanced on the left by the presence of the Al thin layer. Some curvature of the shock front at the edges is evident when it breakout from the foam. This is due to the large foam thickness, which begins to be no longer negligible with respect to the focal spot size. However, the shock front in the central part of the image appears still to be reasonably flat. This was confirmed by performing simulations with the codes MULTI 2D (Ramis & Meyer-ter-Vehn, 1992) and DUED (Atzeni, 1986), by which we also verified that the change in shock velocity

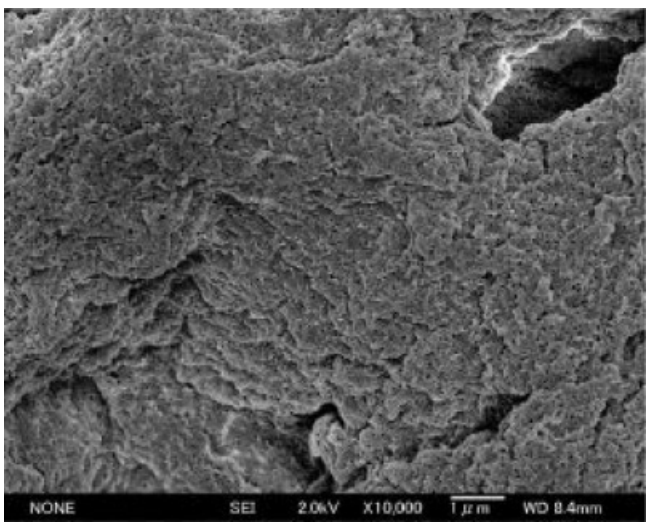

Fig. 8. Scanning electron microscope image of the foams produced at ILE used in the experiment.

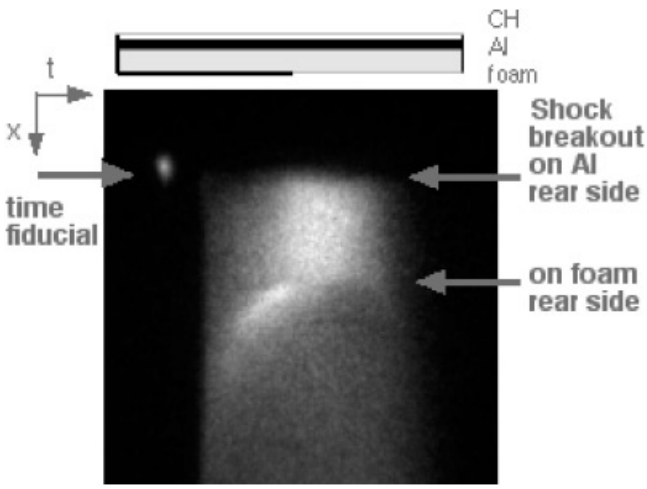

Fig. 9. Shock breakout image from an Al/foam target for laser energy $E_L = 215$ J and a foam density $\rho_o = 0.055$ g/cm^3 (target scheme on the top). Image size is 10 ns $\times$ 1300 μm. Time flows up to down. The time between the fiducial maximum and the breakout on Al rear is $\Delta t = 9$ ps. We did run MULTI simulations by adjusting the laser intensity so to obtain the same fiducial-to-shock delay as in the experiment. These showed that a stationary value of the shock velocity ($D_{Al} = 33.9$ μm/ns) was reached in the last 2 μm of the Al base). The time between shock breakouts on Al and foam is $\Delta t = 3088$ ps giving $D_{foam} = 59.9$ μm/ns (foam thickness was 185 μm on this shot).

https://doi.org/10.1017/S0263034607070164 Published online by Cambridge University Press

with respect to the 1D case is negligible in our experimental conditions. They also allowed checking that the shock velocity is stationary in the foam.

From our experimental results, it was also possible to deduce the acceleration factor ($g = U_{\mathrm{foam}}/U_{\mathrm{Al}}$) vs. foam density (see Fig. 10). We compared our results to two different models. The first calculates the isentropic release curve, in the perfect gas approximation, of the Al plasma in the foam (Teyssier *et al*., 2000). In this case the acceleration factor g must be calculated semi-analytically, as described by Koenig *et al*. (1999*b*). The second one is a simple model based on the fact that, in first approximation, the release curve of Al is symmetric to the cold Huguenot. Thereby this model applies to the case of cold materials and weak shocks (Batani *et al*., 2001; Zeldovich & Raizer, 1967). In this last model, the acceleration factor is simply given by $g = 2(1 + (\rho_{o,\mathrm{foam}}/\rho_{\mathrm{o,Al}})^{0.5})$.

Our results (Dezulian *et al*., 2006) clearly show a much better agreement with the isentropic model. This is due to the fact that in the case of strong shocks, the limiting velocity of expansion of the free surface in a vacuum is larger than what is found for cold materials and weak shocks, that is, $2U_{\mathrm{Al}}$.

SMOOTHING BY FOAMS AND GAS JETS

Apart from their use in astrophysical-dedicated experiments, low-density foams are largely studied because they have the potential of allowing the improvement of target design in ICF (Desselberger *et al*., 1995). This is the main motivation explaining the recent large interest in laser-plasma experiments using foam targets. Indeed, laser imprint may be strongly reduced by thermal smoothing in a relatively-thick, hot, low-density (but over critical) outer foam layer of ICF targets (Batani *et al*., 2000*a*; Dunne *et al*., 1995; Hall *et al*., 2002; Nishimura *et al*., 2000; Limpouch *et al*., 2005). Alternatively, very-low-density (under critical, thin, and transparent) foams may reduce the imprint problem by acting as dynamic phase plates (Limpouch *et al*., 2004; Gus'Kov *et al*., 2000).

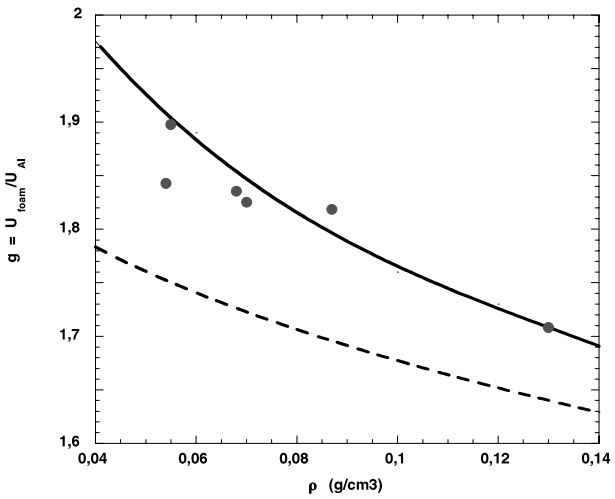

Fig. 10. The acceleration factor ($g = U_{\mathrm{foam}}/U_{\mathrm{Al}}$) from our experimental results (circles) vs. foam density, compared to an "isentropic perfect gas" model (continuous line), and to a "cold material-weak shock" model (Batani *et al*. (2001), dashed line), in which the release isentropic is symmetric to the cold Hugoniot.

Recently however, a new approach to the problem of smoothing has been proposed, namely that of smoothing in a gas jet (Malka *et al*., 2003). In the experiment realized by Malka *et al*. (2003), a laser beam with many speckles was sent through a gas jet and imaged both statically (with a CCD) and dynamically (with a streak camera). Comparison of images before and after passing through a gas jet showed a strong reduction of non-uniformities. Also the authors compared the case in which the gas medium was pre-ionized with an auxiliary laser beam (PP) to the case with no pre-ionization (NPP), and showed that smoothing was sensibly improved in the NPP case. Therefore, they concluded that smoothing was due to a combination of ionization, scattering, and refraction effects.

This seems to be a new promising scheme, not only because of the results obtained by Malka *et al*. (2003), but also because of its intrinsic simplicity. However the experiment was lacking the measurements of the coupling to a target and on assessing real effect on payload hydrodynamics. This is what we realized in a preliminary experiment done at PALS.

In order to perform such kind of experiment, we do need non-uniform irradiation conditions. Therefore, we deliberately didn't use PZPs. Also, of course, well reproducible and known non-uniformities, would of course facilitate the experiment and, finally, we would ideally like to have a 1D modulation in order to be able to compare our experimental results with theoretical analytical models. In a first experiment, we realized such condition by putting a prism on half of the laser beam. This deviated half of the beam producing a double-spot in the focal plane. By adjusting the target plane, we could obtain two focal spots with diameter ≈ 50 μm separated by ≈ 100 μm. Therefore we did produce a *very-large* irradiation non-uniformity, which is *a-priori* very difficult to be smoothed.

At PALS, first we did perform shots on pure Al and foam/Al layered targets in order to compare the shock breakout and see the occurrence of any smoothing effect. To our initial surprise, we observed that streak camera images seem to show a lager smoothing with pure Al targets. Although such results are preliminary, and certainly deserve a more detailed analysis, it can indeed be seen in Figure 11 that the shock breakout in presence of the foam is delayed (as it should be due to the additional thickness), but the "dip" between the two spots seems to be deeper. A possible interpretation of such experimental result is that, under the irradiation conditions at PALS, *radiation* smoothing is dominant due to the strong X-ray preheating. A foam layer on the laser side reduces X-ray generation and radiation preheating. (Let's notice however that, unlike foam or gas smooth-

https://doi.org/10.1017/S0263034607070164 Published online by Cambridge University Press

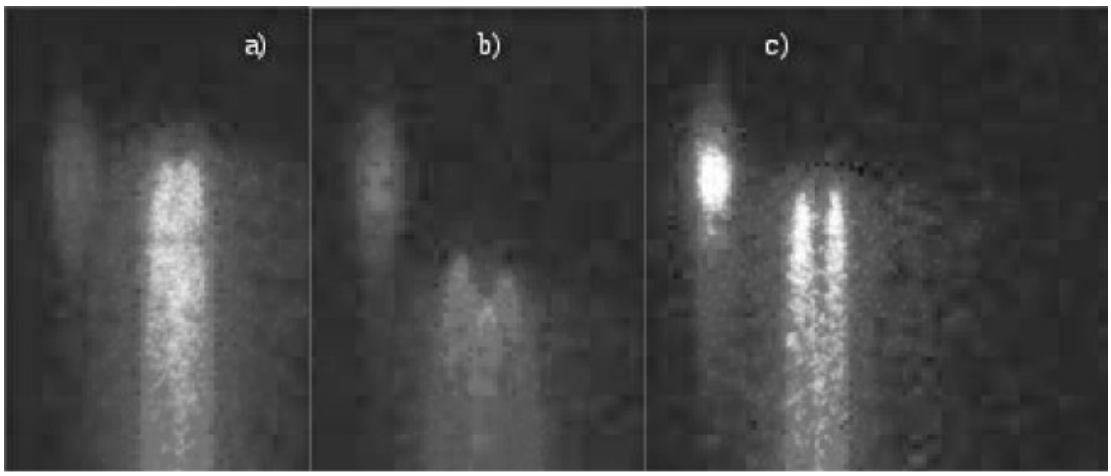

Fig. 11. shock breakout images from pure Al and foam/Al targets: (**a**) $E = 49$ J, Al 10 μm; (**b**) $E = 48$ J, foam 50 μm 50 g/cm^3 and Al 10 μm; (**c**) $E = 9$ J, Al 10 μm. Images dimensions: 2 ns $\times$ 1300 μm.

ing, radiation smoothing is not beneficial for ICF implying a large target preheating.) The image in Figure 11c gives a support to such interpretation. At lower laser energy, X-ray generation is strongly reduced and the two shock breakouts from the two focal spots return to be well separated.

The reasons for such large preheating, as compared for instance, to the measurements by Batani *et al*. (2000*a*), probably lie in the use of very short wavelength laser radiation (which is known to increase X-ray generation), and in the fact that we did not use a CH layer before the Al target in order to reduce X-ray generation.

After the foam shots, we used an Ar gas jet placed before the target to test the gas-smoothing approach. As with Malka *et al*. (2003), we obtained static and dynamical images and compared them with and without gases. Our typical results, shown in Figure 12, show that in the presence of gas, the space between the two focal spots is *filled-in*, i.e., the non-uniformity are strongly reduced.

We also studied the coupling of the laser beam with/without the gas jet to a payload target (Al 10 μm) by using our time-resolved self-emission diagnostics again, i.e., by analyzing the shock breakout from the rear side of the target

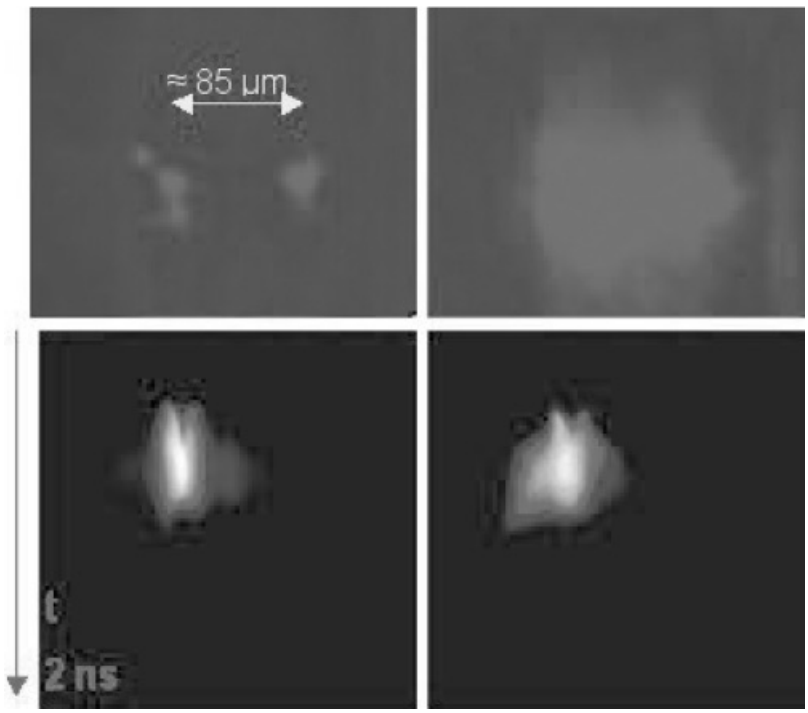

Fig. 12. Gas Jet experiment at PALS, Focal Spot. Static images (up): no gas (left), Ar 5 bar (right). Dynamic images (bottom): no gas (left); Ar 5 bar (right).

https://doi.org/10.1017/S0263034607070164 Published online by Cambridge University Press

at different gas jet pressures. Our results are shown in Figure 13.

We clearly see two effects. First, the shock breakout is delayed when the gas pressure is increased. This corresponds to reduced laser intensity on target (therefore a reduced shock pressure and shock velocity) because of the losses of energy in gas ionization, and because the smoothing effect distributes the energy on a larger area, thereby decreasing intensity (sees also Fig. 11). The weaker shock also corresponds to a reduced temperature and therefore a weaker emissive when it reaches the target rear side, an effect that is evident in Figure 12.

Second, the non-uniformity is strongly decreased in the presence of the gas jet. Let's notice that images obtained with Ar gas pressure ≤ 1 bar do not differ form images obtained without gas; therefore 1 bar seems to be too low to produce any appreciable smoothing effect (gas density too low). Above 10 bar, the streak camera does not show any shock breakout image: the shock clearly becomes too weak (not much self-emission), and too slow (it may fall outside the observation temporal window).

Finally let's notice that in our experiment, we used Ar as the gas medium, while He was used by Malka *et al*. (2003). In our case, no effect was observed with He. This is certainly due to the fact that we used very large non-uniformities, while non-uniformities by Malka *et al*. (2003) were of a few microns only. Therefore, a much larger plasma density is needed to produce an appreciable diffusion/refraction.

In a following experiment, we plan to produce more 1D (i.e., we want a focal spot which has modulation in intensity in only one direction) and shorter wavelength non-uniformities. We plan to this either by using a mask placed on the laser beam outside the interaction chamber, or by using a phase plate of new conception (D. Pepler, private communication) which has been designed to produce stripes of about 40 μm width over a focal spot with overall dimension about 400 μm $\times$ 400 μm. We have already performed some preliminary tests with both approaches. In the first approach (mask) of course the target must be placed outside of the focal plane, where to far-field diffraction effects the modulations are lost. We are then forced to work in an intermediate plane (not far-field, not near-field) where the laser intensity is still high enough to produce an intense plasma while maintaining the modulations. Indeed this is possible thanks to the very high laser energy per shot, which is available on PALS. Intensities in the order of 10^{14} W/cm^2 (which are required for this kind of experiments) can still be obtained while defocusing the beam of about 1 mm.

In order to check if the method works, we imaged the focal spot in static and dynamical mode (see Fig. 14). The results clearly show the presence of a "stripy" focal spot. The "hole" in the centre of the first image in Figure 14 is due to the initial near-field distribution of laser energy in the PALS beam (stronger at the edges) and also to the presence of a hole in the main focusing lens (introduced to avoid multiple reflections inside the lens which could induce it to break). In the second approach (new phase plate), we have impacted the laser beam on a thick Al target (100 μm) at low intensity (5 J on target). The resulting ablation impact (see Fig. 15) clearly shows the presence of a "stripy" focal spot.

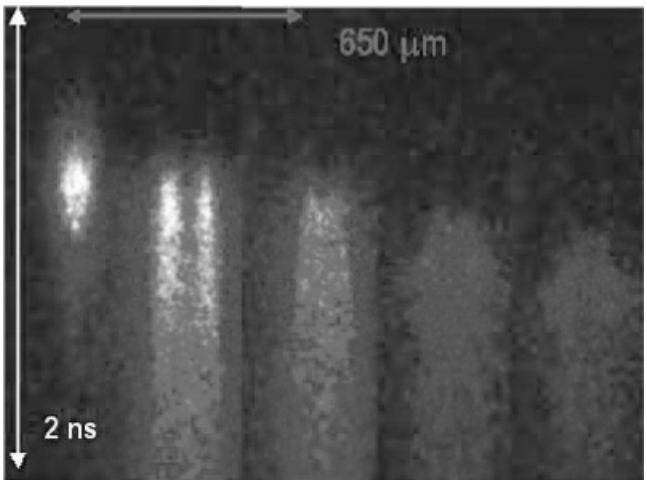

Fig. 13. shock breakout images from the double focal spot on a 10 μm Al target. From left to right: 1 bar (as in vacuum) 18 J; 2 bar 18 J; 5 bar 18 J; 10 bar 25 J.

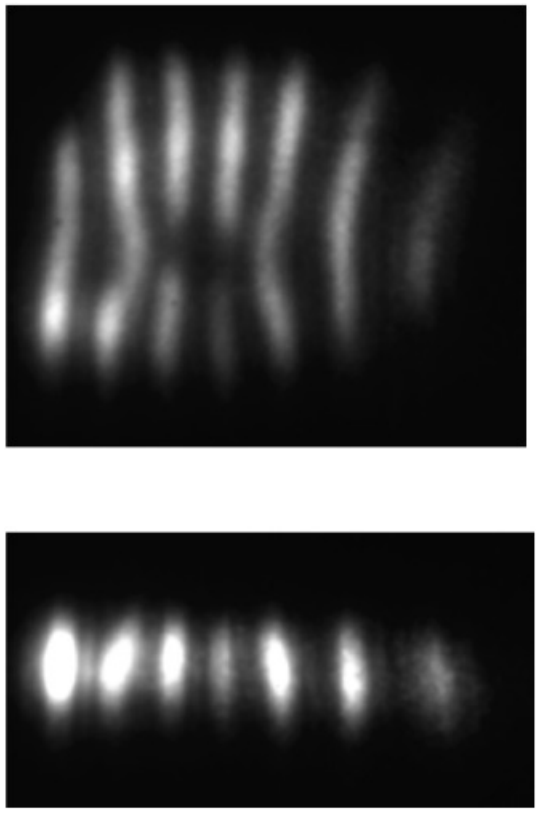

Fig. 14. Static (up, CCD) and dynamic (down, streak camera) images of the stripy focal spot obtained with the mask. The horizontal linear dimension of the static image is about 500 μm.

https://doi.org/10.1017/S0263034607070164 Published online by Cambridge University Press

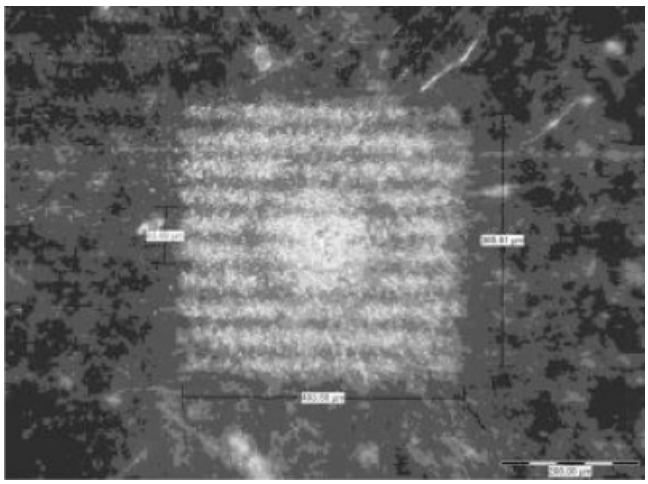

Fig. 15. Ablation impact obtained with a low energy shot using the new phase plate on a thick Al target.

CONCLUSIONS

Progress in laser technology allows realizing *cleaner* experiments, and conditions closer to those for which theoretical models have been derived. In particular, laser smoothing techniques like PZPs allows to improve irradiation conditions by getting an almost uniform intensity profile, strongly reducing 2D effects (lateral transport of thermal energy, lateral flow of mass).

We have presented a series of experiments respectively dedicated to the study of shock (ablation) pressures vs. laser intensity; the generation of extreme states of matter by laser compression, and the application to the study of EOS of material in the Mbar pressure range (here we have used carbon); the study of shock acceleration in foams (a problem which is important also in connection to astrophysical situations); and finally the study of smoothing of laser energy deposition by foams and gas jets.

Concerning shock pressure, our results show a scaling vs. laser intensity, which is quite close to the theoretical prediction and gives some evidence for the mechanism of delocalized absorption.

Concerning the EOS of carbon, we have obtained the first Huguenot data for carbon with laser-driven shocks and got the first experimental points at pressures higher than 8 Mbar. Moreover, we substantially increased the number of EOS data for carbon at pressures >1 Mbar.

Concerning the problem of the shock-induced acceleration when the shock crosses the Al/foam interface, we performed some measurements by changing foam density and showed that results are in close agreement with the predictions from a theoretical model, which calculates the isentropic release in the perfect gas approximation (Fabbro *et al*., 1982, 1985; Garban-Labaune *et al*., 1985; Zeldovich & Raizer, 1967).

Concerning the experiment on smoothing of laser nonuniformities in a gas jet, we saw that the gas jets give good smoothing effect: very large non-uniformities seem to be smoothed very effectively.

In conclusion, we have shown that laser-plasmas are a very interesting tool for the study of some hydrodynamical problems and their applications. Also, using laser facilities like PALS, it is possible to perform many interesting and useful experiments in plasma physics

ACKNOWLEDGMENTS

The authors thank the technical staffs of PALS for help in running the experiments. Special thanks at B. Kralikova, Ch. Kadlec, T. Mocek, A. Präg, J. Polan, M. Kozlová, M. Stupka, P. Homer, T. Havlicek, M. Soukup from PALS, and S. Barbanotti, F. Orsenigo, T. Vinci, A. Ravasio, C. Olivotto, E. Henry, M. Moret from the University of Milano Bicocca. We acknowledge useful discussion with R. Ramis (Universidad Politecnica, Madrid), S. Atzeni (Università La Sapienza, Rome), and the help of J. Kaae (General Atomics, San Diego, USA), F. Ito and Y. Ochi (ILE, Osaka University), P. Milani, E. Barborini, P. Piseri (Università di Milano), and S. Alba (ST, Agrate Brianza) for the work on target production and/or characterization. We thank J. Meyer-ter-Vehn and A. Kemp for the availability of the QEOS code (in the version MPQEOS developed at MPQ). The work supported by the European Union under contract HPRI-CT-1999-00053 Transnational Access to Major Research Infrastructures (ARI) of 5th FP and the "LaserLab" program of the sixth FP.

REFERENCES

Ancilotto, F., Chiarotti, G.L., Scandolo, S. & Tosatti, E. (1997). dissociation of methane into hydrocarbons at extreme (planetary) pressure and temperature. *Science* **275**, 1288–1290.

Atzeni, S. (1986). 2-D Lagrangian studies of symmetry and stability of laser fusion targets. *Comp. Phys. Commun.* **43**, 107–124.

Barborini, E., Piseri, P. & Milani, P. (1999). A pulsed microplasma source of high intensity supersonic carbon cluster beams. *J. Phys. A* **32**, L105–L109.

Barborini, E., Piseri, P., Podesta, A. & Milani, P. (2000). Cluster beam microfabrication of patterns of three-dimensional nanostructured objects. *Appl. Phys. Lett.* **77**, 1059–1061.

Batani, D., Balducci, A., Nazarov, W., Löwer, T., Hall, T., Koenig, M., Faral, B., Benuzzi, A. & Temporal, M. (2001). Use of low-density foams as pressure amplifiers in equation-of-state experiments with laser-driven shock waves. *Phys. Rev. E* **63**, 046410–420.

Batani, D., Balducci, A., Beretta, D., Bernardinello, A., Löwer, T., Koenig, M., Benuzzi, A., Faral, B. & Hall, T. (2000*b*). Equation of state data for gold in the pressure range <10 TPa. *Phys. Rev. B* **61**, 9287–9294.

Batani, D., Barbanotti, S., Canova, F., Dezulian, R., Stabile, H., Ravasio, A., Lucchini, G., Ullschmied, J., Krousky, E., Skala, J., Juha, L., Kralikova, B., Pfeifer, M., Kadlec, C., Mocek, T., Prag, A., Nishimura, H. & Ochi, Y. (2004*a*). Laser driven shock experiments at PALS. *Czech. J. Phys.* **54**, 431–443.

Batani, D., Bleu, C. & Löwer, T. (2002*a*). Design, simulation and application of phase plates. *Euro. Phys. J. D* **19**, 231–243.

https://doi.org/10.1017/S0263034607070164 Published online by Cambridge University Press

Batani, D., Morelli, A., Tomasini, M., Benuzzi-Mounaix, A., Philippe, F., Koenig, M., Marchet, B., Masclet, I., Rabec, M., Reverdin, Ch., Cauble, R., Celliers, P., Collins, G., Da Silva, L., Hall, T., Moret, M., Sacchi, B., Baclet, P. & B. Cathala, B. (2002*b*). Equation of state data for iron at pressures beyond 10 Mbar. *Phys. Rev. Lett.* **88**, 235502–505.

Batani, D., Nazarov, W., Hall, T., Löwer, T., Koenig, M., Faral, B., Benuzzi-Mounaix, A. & Grandjouan, N. (2000*a*). Foam-induced smoothing studied through laser-driven shock waves. *Phys. Rev. E* **62**, 8573–8582.

Batani, D., Stabile, H., Ravasio, A., Desai, T., Lucchini, G., Desai, T., Ullschmied, J., Krousky, E., Juha, L., Skala, J., Kralikova, B., Pfeifer, M., Kadlec, C., Mocek, T., Präg, A., Nishimura, H. & Ochi, Y. (2003*a*). Ablation pressure scaling at short laser wavelength. *Phys. Rev. E* **68**, 067403–406.

Batani, D., Stabile, H., Tomasini, M., Lucchini, G., Ravasio, A., Koenig, M., Benuzzi-Mounaix, A., Nishimura, H., Ochi, Y., Ullschmied, J., Skala, J., Kralikova, B., Pfeifer, M., Kadlec, Ch., Mocek, T., Präg, A., Hall, T., Milani, P., Barborini, E. & Piseri, P. (2004*b*). Huguenot data for carbon at megabar pressures. *Phys. Rev. Lett.* **92**, 065503.

Batani, D., Strati, F., Telaro, B., Löwer, T., Hall, T., Benuzzi-Mounaix, A. & Koenig, M. (2003*b*). Production of high quality shocks for equation of state experiments. *Euro. Phys. J D* **23**, 99–107.

Benedetti, L.R., Nguyen, J.H., Caldwell, W.A., Liu, H., Kruger, M. & Jeanloz, R. (1999). Dissociation of CH_4 at high pressures and temperatures: Diamond formation in giant planet interiors? *Science* **286**, 100–102.

Benuzzi, A., Koenig, M., Faral, B., Krishnan, J., Pisani, F., Batani, D., Bossi, S., Beretta, D., Hall, T., Ellwi, S., Hüller, S., Honrubia, J. & Grandjouan, N. (1998). Pre-heating study by reflectivity measurements in laser-driven shocks. *Phys. Plasmas* **5**, 2410–2420.

Benuzzi-Mounaix, A., Koenig, M., Boudenne, J.M., Hall, T.A., Batani, D., Scianitti, F., Masini, A. & DiSanto, D. (1999). Chirped pulse reflectivity and frequency domain interferometry in laser driven shock experiments. *Phys. Rev. E* **60**, R2488–R2491.

Bundy, F.P. (1963). Direct conversion of graphite to diamond in static pressure apparatus. *J. Chem. Physics* **38**, 631–643.

Bundy, F.P. (1989). Pressure-temperature phase diagram of elemental carbon. *Phys. A* **156**, 169–178.

Bundy, F.P., Strong, H.M. & Wentorf, R.H. (1973). Methods and mechanisms of synthetic diamond growth. In *Chemistry and Physics of Carbon* (Thrower, P.A., Ed.). New York: Decker.

Caruso, A. & Gratton, R. (1968). Some properties of the plasmas produced by irradiating light solids by laser pulses. *Plasma Phys.* **10**, 867–877.

Cavalleri, A., Sokolowski-Tinten, K., von der Linde, D., Spagnolatti, I., Bernasconi, M., Benedek, G., Podestà, A. & Milani, P. (2002). Generation of the low-density liquid phase of carbon by non-thermal melting of fullerene. *Europhys. Lett.* **57**, 281.

Chizhkov, M.N., Karlykhanov, N.G., Lykov, V.A., Shushlebin, A.N., Sokolov, L. & Timakova, M.S. (2005). Computational optimization of indirect-driven targets for ignition on the Iskra-6 laser facility. *Laser Part. Beams* **23**, 261–265.

Ciardi, A., Lebedev, S.V., Chittenden, J.P. & Bland, S.N. (2002). Modeling of supersonic jet formation in conical wire array Z-pinches. *Laser Part. Beams* **20**, 255–261.

Connerney, J.E.P., Acuna, M.H. & Ness, N.F. (1987). The magnetic field of Uranus. *J. Geophys. Rev.* **92**, 15329.

Desai, T., Dezulian, R. & Batani, D. (2007). Radiation effects on shock propagation in Aluminum target relevant to EOS measurements. *Laser Part. Beams* **25**, 23–30.

Desselberger, M., Jones, M.W., Edwards, J., Dunne, M. & Willi. O. (1995). Use of X-ray preheated foam layers to reduce beam structure imprint in laser-driven targets. *Phys. Rev. Lett.* **74**, 2961–2964.

Dezulian, R., Canova, F., Barbanotti, S., Orsenigo, F., Redaelli, R., Vinci, T., Lucchini, G., Batani, D., Rus, B., Polan, J., Kozlová, M., Stupka, M., Praeg, A.R., Homer, P., Havlicek, T., Soukup, M., Krousky, E., Skala, J., Dudzak, R., Pfeifer, M., Nishimura, H., Nagai, K., Ito, F., Norimatsu, T., Kilpio, A., Shashkov, E., Stuchebrukhov, I., Vovchenko, V., Chernomyrdin, V. & Krasuyk, I. (2006). Huguenot Data of Plastic Foams obtained from Laser-Driven Shocks. *Phys. Rev. E* **73**, 047401–404.

Drake, R.P. (2005). Hydrodynamic instabilities in astrophysics and in laboratory high energy–density systems. *Plasma Phys. Contr. Fusion* **47**, B419–B440.

Drakin, V.P. & Pavlovskii, M.N. (1966). Concerning the metallic phase of carbon (Ceylon and artificial graphite behavior under very high pressure, examining problem of metallic phase of carbon). *JETP Lett* **4**, 116–118.

Dunne, M., Borghesi, M., Iwase, A., Jones, M.W., Taylor, R., Willi, O., Gibson, R., Goldman, S.R., Mack, J. & Watt, R.G. (1995). Evaluation of a foam buffer target design for spatially uniform ablation of laser-irradiated plasmas. *Phys. Rev. Lett.* **75**, 3858–3861.

Eidmann, K., Bar-Shalom, A., Saemann, A. & Winhart, G. (1998). Measurement of the extreme UV opacity of a hot dense gold plasma. *Europhys. Lett.* **44**, 459–464.

Eliezer, S., Ghatak, A. & Hora, H. (1986). *Equation of State: Theory and Applications*. Cambridge, UK: Cambridge University Press.

Fabbro, R., Faral, B., Virmont, J., Cottet, F., Romain, J.P. & Pépin, H. (1985). Experimental study of ablation pressures and target velocities obtained in 0.26 μm wavelength laser experiments in planar geometry. *Phys. Fluids* **28**, 3414–3423.

Fabbro, R., Fabre, E., Amiranoff, F., Garban-Labaune, C., Virmont, J., Weinfeld, M. & Max, C.E. (1982). Laser-wavelength dependence of mass-ablation rate and heat-flux inhibition in laser-produced plasmas. *Phys. Rev. A* **26**, 2289–2292.

Fahy, S. & Louie, S.G. (1987). High-pressure structural and electronic properties of carbon. *Phys. Rev. B* **36**, 3373–3385.

Fincke, J.R., Lanier, N.E., Batha, S.H., Hueckstaedt, R.M., Magelssen, G.R., Rothman, S.D., Parker, K.W. & Horsfield, C. (2005). Effect of convergence on growth of the Richtmyer-Meshkov instability. *Laser Part. Beams* **23**, 21–25.

Fleury, X., Bouquet, S., Stehle, C., Koenig, M., Batani, D., Benuzzi-Mounaix, A., Chieze, J.P., N.Grandjouan, Grenier, J., Hall, T., Enry, E., Lafon, J.P., Leygnac, S., Malka, V., Marchet, B., Merdij, H., Michaut, C. & Thais, F. (2002). A laser experiment for studying radiative shocks in astrophysics. *Laser Part. Beams* **20**, 263–268.

Garban-Labaune, C., Fabre, E., Max, C., Amiranoff, F., Fabbro, R., Virmont, J. & Mead, W.C. (1985). Experimental

https://doi.org/10.1017/S0263034607070164 Published online by Cambridge University Press

results and theoretical analysis of the effect of wavelength on absorption and hot-electron generation in laser-plasma interaction. *Phys. Fluids* **28**, 2580–2590.

Grumbach, M.P. & Martin, R.M. (1996). Phase diagram of carbon at high pressures and temperatures. *Phys. Rev. B* **54**, 15730–15741.

Guillot, T. (1999). Interiors of giant planets inside and outside the solar system. *Science* **286**, 72–77.

Gupta, Y.M. & Sharma, S.M. (1997). Shocking matter to extreme conditions. *Science* **277**, 909–910.

Gus'Kov, SY. (2005). Thermonuclear gain and parameters of fast ignition ICF-targets. *Laser Part. Beams* **23**, 255–260.

Gus'Kov, S.Y., Gromov, A.I., Merkul'ev, Yu.A., Rozanov, V.B., Nikishin, V., Tishkin, V.F., Zmitrenko, N.V., Gavrilov, V.V., Gol'tsov, A.A., Kondrashov, V.N., Kovalsky, N.V., Pergament, M.I., Garanin, S.G., Kirillov, G.A., Sukharev, S.A., Caruso, A. & Strangio, C. (2000). Nonequilibrium laser-produced plasma of volume-structured media and ICF applications. *Laser Part. Beams* **18**, 1–10.

Gust, W.H. (1980). Phase transition and shock-compression parameters to 120 GPa for three types of graphite and for amorphous carbon. *Phys. Rev. B* **22**, 4744–4756.

Hall, T., Batani, D., Nazarov, W., Koenig, M. & Benuzzi, A. (2002). Recent advances in laser–plasma experiments using foams. *Laser Part. Beams* **20**, 303–316.

Hoffmann, D.H.H., Blazevic, A., Ni, P., Rosmej, O., Roth, M., Tahir, N.A., Tauschwitz, A., Udrea, S., Varentsov, D., Weyrich, K. & Maron, Y. (2005). Present and future perspectives for high energy density physics with intense heavy ion and laser beams. *Laser Part. Beams* **23**, 47–53.

Hora, H. (2006). Smoothing and stochastic pulsation at high power laser-plasma interaction. *Laser Part. Beams* **24**, 455–463.

Jungwirth, K. (2005). Recent highlights of the PALS research program. *Laser Part. Beams* **23**, 177–182.

Jungwirth, K., Cejnarova, A., Juha, L., Kralikova, B., Krasa, J., Krousky, E., Krupickova, P., Laska, L., Masek, K., Mocek, T., Pfeifer, M., Präg, A., Renner, O., Rohlena, K., Rus, B., Skala, J., Straka, P. & Ullschmied, J. (2001). The Prague Asterix Laser System. *Phys. Plasmas* **8**, 2495–2501.

Kato, Y., Mima, K., Miyanaga, N., Arinaga, S., Kitagawa, Y., Nakatsuka, M. & Yamanaka, C. (1984). Random phasing of high-power lasers for uniform target acceleration and plasma-instability suppression. *Phys. Rev. Lett.* **53**, 1057–1060.

Key, M.H., Rumsby, P.T., Evans, R.G., Lewis, C.L.S., Ward, J.M. & Cooke, R.L. (1980). Study of Ablatively Imploded Spherical Shells. *Phys. Rev. Lett.* **45**, 1801–1804.

Key, M.H., Toner, W.T., Goldsack, T.J., Kilkenny, J.D., Veats, S.A., Cunningham, P.F. & Lewis, C.L.S. (1983). A study of ablation by laser irradiation of plane targets at wavelengths 1.05, 0.53, and 0.35 μm. *Phys. Fluids* **26**, 2011–2026.

Kilkenny, J.D., Alexander, N.B., Nikroo, A., Steinman, D.A., Nobile, A., Bernat, T., Cook, R., Letts, S., Takagi, M. & Harding, D. (2005). Laser targets compensate for limitations in inertial confinement fusion drivers. *Laser Part. Beams* **23**, 475–482.

Koenig, M., Benuzzi, A., Faral, B., Batani, D., Muller, L., Torsiello, F., Hall, T., Grandjouan, N. & Nazarov, W. (2000). EOS data for CH foams using smoothed laser beams. *Astro. J.* **127**, 385.

Koenig, M., Benuzzi, A., Philippe, F., Batani, D., Hall, T., Grandjouan, N. & Nazarov, W. (1999*a*). Equation of state data experiments for plastic foams using smoothed laser beams. *Phys. Plasmas* **6**, 3296–3301.

Koenig, M., Benuzzi-Mounaix, A., Batani, D., Hall, T. & Nazarov, W. (2005*b*). Shock velocity and temperature measurements of plastic foams compressed by smoothed laser beams. *Phys. Plasmas* **12**, 012706–711.

Koenig, M., Benuzzi-Mounaix, A., Philippe, F., Faral, B., Batani, D., Hall, T.A., Grandjouan, N., Nazarov, W., Chieze, J.P. & Teyssier, R. (1999*b*). Laser driven shock wave acceleration experiments using plastic foams. *Appl. Phys. Lett.* **75**, 3026–3028.

Koenig, M., Faral, B., Boudenne, J.M., Batani, D., Benuzzi, A., Bossi, S., Rémond, C., Perrine, J.P., Temporal, M. & Atzeni, S. (1995). Relative consistency of equations of state by laser driven shock waves. *Phys. Rev. Lett.* **74**, 2260–2263.

Koenig, M., Faral, B., Boudenne, J.M., Batani, D., Benuzzi, A. & Bossi, S. (1994). Optical smoothing techniques for shock wave generation in laser-produced plasmas. *Phys. Rev. E* **50**, R3314–R3317.

Koenig, M., Fabre, E., Malka, V., Michard, A., Hammerling, P., Batani, D., Boudenne, J.M., Garconnet, J.P. & Fews, P. (1992). Recent results on implosions directly driven at lambda = 0.26-m laser wavelength. *Laser Part. Beams* **10**, 573.

Koenig, M., Vinci, T., Benuzzi-Monnaix, A., Lepape, S., Ozaki, N., Bouquet, S., Boireau, L., Leygnac, S., Michaut, C., Stehle, C., Chieze, J.P., Batani, D., Hall, T., Tanaka, K. & Yoshida, M. (2005*a*). Radiative shock experiments at LULI. *Astrophys. Space Sci.* **298**, 69–74.

Koenig, M., Vinci, T., Benuzzi-Mounaix, A., Ozaki, N., Ravasio, A., Boireau, L., Michaut, C., Bouquet, S., Atzeni, S., Schiavi, A., Peyrusse, O., Batani, D., Drake, R.P. & Reighard, A.B. (2006). Radiative shocks: An opportunity to study laboratory astrophysics. *Phys. Plasmas* **13**, 056504.

Koresheva, E.R., Osipov, I.E. & Aleksandrova, I.V. (2005). Free standing target technologies for inertial fusion energy: Target fabrication, characterization, and delivery. *Laser Part. Beams* **23**, 563–571.

Lebo, I.G., Yu, A.M., Tishkin, V.F. & Zvorykin, V.D. (1999). Analysis and 2D numerical modeling of burn through of metallic foil experiments using power KrF and Nd lasers *Laser Part. Beams* **17**, 753–758.

Limpouch, J., Demchenko, N.N., Gus'Kov, S.Y., Gromov, A.I., Kalal, M., Kasperczuk, A., Kondrashov, V.N., Krousky, E., Masek, K., Pfeifer, M., Pisarczyk, P., Pisarczyk, T., Rohlena, K., Rozanov, V.B., Sinor, M. & Ullschmied, J. (2005). Laser interactions with low-density plastic foams. *Laser Part. Beams* **23**, 321–325.

Limpouch, J., Demchenko, N.N., Gus'Kov, S.Y., Kálal, M., Kasperczuk, A., Kondrashov, V.N., Krouski, E., Masek, K., Pisarczyk, P., Pisarczyk, T. & Rozanov, V.B. (2004). Laser interactions with plastic foam—metallic foil layered targets. *Plasma Phys. Contr. Fusion* **46**, 1831–1841.

Lindl, J. (1995). Development of the indirect-drive approach to inertial confinement fusion and the target physics basis for ignition and gain. *Phys. Plasmas* **2**, 3933–4024.

Malka, V., Faure, F., Huller, S., Tikhonchuk, V.T., Weber, S. & Amiranoff, F. (2003). Enhanced spatiotemporal laser-beam smoothing in gas-jet plasmas. *Phys. Rev. Lett.* **90**, 075002.

Mao, H.K. & Bell, P.M. (1978). High-pressure physics: Sustained static generation of 1.36 to 1.72 Megabars. *Science* **200**, 1145–1147.

Mao, H.K. & Bell, P.M. (1979). Observations of hydrogen at room temperature (25°C) and high pressure (to 500 Kilobars). *Science* **203**, 1004–1006.

Mao, H.K. & Hemley, R.J. (1991). Optical transitions in diamond at ultrahigh pressures. *Nature* **351**, 721–724.

Marsh, S.P. (1980). *LASL Shock Huguenot Data*, pp. 28–51. Berkeley, CA: University of California, Berkeley, 28–51.

Meyer, B. & Thiell, G. (1984). Experimental scaling laws for ablation parameters in plane target–laser interaction with 1.06 μm and 0.35 μm laser wavelengths. *Phys. Fluids* **27**, 302–311.

Mora, P. (1982). Theoretical model of absorption of laser light by a plasma. *Phys. Fluids* **25**, 1051–1056.

More, R.M., Warren, K.H., Young, D.A. & Zimmerman, G.B. (1988). A new quotidian equation of state (QEOS) for hot dense matter. *Phys. Fluids* **31**, 3059–3078.

Nagai, K., Cho, B.-R., Hashishin, Y., Norimatsu, T. & Yamanaka, T. (2002*a*). Microstructures of ultralow-density foam plastics obtained by altering the coagulant alcohol. *Jp. J. Appl. Phys.* **41**, L431–L433.

Nagai, K., Norimatsu, T., Yamanaka, T., Nishibe, T., Ozaki, N., Takamatsu, K., Ono, T., Nakano, M. & Tanaka, K.A. (2006*b*). Single molecular membrane glue technique for laser driven shock experiments. *Jp. J. Appl. Phys.* **41**, L1184–L1186.

Nagai, K., Takayoshi, N. & Yasukazu, I. (2004). Control of micro- and nano-structure in ultra low-density hydrocarbon foam. *Fusion Sci. Technol.* **45**, 79–83.

Nellis, W.J., Hamilton, D.C., Holmes, N.C., Radousky, H.B., Ree, F.H., Mitchell, A.C. & Nicol, M. (2001*a*). Nature of the interior of Uranus based on studies of planetary ices at high dynamic pressure. *Science* **240**, 779–781.

Nellis, W.J., Mitchell, A.C. & McMahan, A.K. (2001*b*). Carbon at pressures in the range 0.1–1 TPa (10 Mbar). *J. Appl. Phys.* **90**, 696–698.

Ness, N.F., Acuna, M.H., Behannon, K.W., Burlaga, L.F., Connerney, J.E.P. & Lepping, R.P. (1986). Magnetic fields at Uranus. *Science* **233**, 85–89.

Nishimura, H., Shiraga, H., Azechi, H., Miyanaga, N., Nakai, M., Izumi, N., Nishikino, M., Heya, M., Fujita, K., Ochi, Y., Shigemori, K., Ohnishi, N., Murakami, M., Nishihara, K., Ishizakia, R., Takabe, H., Nagai, K., Norimatsu, T., Nakatsuka, M., Yamanaka, T., Nakai, S., Yamanakab, C. & Mima, K. (2000). Indirect-direct hybrid target experiments with the GEKKO XII laser. *Nucl. Fusion* **40**, 547–556.

Okihara, S., Esirkepov, T.Zh., Nagai, K., Shimizu, S., Sato, F., Hashida, M., Iida, T., Nishihara, K., Norimatsu, T., Izawa, Y. & Sakabe, S. (2004). Ion generation in a low-density plastic foam by interaction with intense femtosecond laser pulses. *Phys. Rev. E* **69**, 026401–404.

Pant, H.C., Shukla, M., Pandey, H.D., Kashyap, Y., Sarkar, P.S., Sinha, A., Senecham, V.K. & Godwal, B.K. (2006). Enhancement of laser induced shock pressure in multilayer solid targets. *Laser Part. Beams* **24**, 169–174.

Pavlovskii, M.N. (1971). Shock compression of diamond. *Soviet Phys. Solid State* **13**, 741.

Piriz, A.R., Cela, J.J.L., Serena Moreno, M.C., Tahir, N.A. & Hoffmann, D.H.H. (2006). Thin plate effects in the Rayleigh-Taylor instability of elastic solids. *Laser Part. Beams* **24**, 275–282.

Piseri, P., Podestà, A., Barborini, E. & Milani, P. (2001). Production and characterization of highly intense and collimated cluster beams by inertial focusing in supersonic expansions. *Rev. Sci. Instr.* **72**, 2261–2267.

Ramis, R. & Meyer-ter-Vehn, J. (1992). *MULTI2D-A Computer Code for Two-Dimensional Radiation Hydrodynamics*. Munchen, Germany: Max-Planck-Institut für Quantenoptik.

Ross, M. (1981). The ice layer in Uranus and Neptune—diamonds in the sky? *Nature* **292**, 435–436.

Ross, M. (1985). Matter under extreme conditions of temperature and pressure. *Rtp. Prog. Phys.* **48**, 1–52.

Ruoff, A.L. & Luo, H. (1991). Pressure strengthening: A possible route to obtaining 9 Mbar and metallic diamonds. *J. Appl. Phys.* **70**, 2066.

Saumon, D., Chabrier, G. & Vanhorn, H.M. (1995). An equation of state for low-mass stars and giant planets. *Astrophys. J.* **99**, 713–741.

Scandolo, S., Chiarotti, G.L. & Tosatti, E. (1996). SC4: A metallic phase of carbon at terapascal pressures. *Phys. Rev. B* **53**, 5051–5054.

Sekine, T. (1999). Sixfold-coordinated carbon as a post diamond phase. *Appl. Phys. Lett.* **74**, 350–352.

SESAME. (1983). Report on the Los Alamos equation-of-state library. Report No. LALP-83-4. Los Alamos, NM: Los Alamos National Laboratory.

Stevenson, R.M., Norman, M.J., Bett, T.H., Pepler, D.A., Danson, C.N. & Ross, I.N. (1994). Binary-phase zone plate arrays for the generation of uniform focal profiles. *Opt. Lett.* **19**, 363.

Teyssier, R., Ryutov, D. & Remington, B. (2000). Accelerating shock waves in a laser-produced density gradient, *Astrophys. J.* **127**, 503–508.

Vinci, T., Koenig, M., Benuzzi-Mounaix, A., Boireau, L., Bouquet, S., Leygnac, S., Michaut, C., Stehle, C., Peyrusse, O. & Batani, D. (2005). Density and temperature measurements on laser generated radiative shocks. *Astrophys. Space Sci.* **298**, 333–336.

Winhart, G., Eidmann, H., Iglesias, C.A. & Bar-Shalom, A. (1996). Measurements of extreme uv opacities in hot dense Al, Fe, and Ho. *Phys. Rev. E* **53**, R1332–R1335.

Zeldovich, Y.B. & Raizer, Y.P. (1967). *Physics of Shock Waves and High Temperature Hydrodynamic Phenomena*. New York: Academic Press.